Interpretation of heat-flow density in the Central Andes

Michael Springer [*]

GeoForschungsZentrum Potsdam, Telegrafenberg, 14473 Potsdam, Germany

Abstract

This study focuses on the interpretation of surface heat-flow density data in the central Andes to examine possible lithospheric thermal structures. Along a profile at about 21ºS from the Peru–Chile trench in the west to the Andean foreland in the east, surface heat-flow density is used to constrain quantitative models that are employed to investigate the influence of various effects on the thermal field. Negligible changes in surface heat-flow density along strike of the Andean orogen, in contrast to major variations across the orogen, seem to justify the application of two-dimensional (2-D) cross-section models. The region of the Andean orogen between the trench and the volcanic front is described by 2-D subduction models, the back-arc region, characterised by crustal doubling, is analysed by 2-D models describing simple underthrust phenomena and the Andean foreland is investigated by one-dimensional temperature estimates. The influence of various geometrical and petrophysical parameters on the thermal structure is investigated. Model calculations show that the low heat-flow density values in the fore-arc region suggest low shear stresses on the order of 15 MPa along the plate contact. Variations of the subduction angle influence mainly the W–E extent of the surface heat-flow density anomaly. The distribution of the crustal radiogenic heat-production rate influences the surface heat-flow density significantly, but has only a minor influence on crustal temperatures. Modelling results show that temperatures at the maximum depth of seismic coupling between the oceanic Nazca plate and the overriding South American continental plate ($\sim$45 km) are on the order of 250 to 300ºC, whereas at the maximum depth of the plate contact ($\sim$60 km) temperatures are on the order of 300 to 350ºC. The lithospheric temperature structure in the active magmatic arc region is strongly sensitive to temperature changes caused by the occurrence of an assumed asthenospheric mantle wedge at shallow depth ($\sim$70 km). To match conditions for melting at subcrustal levels, the minimum extent of an asthenospheric wedge towards the west has to coincide with the position of the volcanic front. The thermally thinned lithosphere results in a surface heat-flow density on the order of 60–70 mW m^{-2}. Locally higher heat-flow density in the volcanic arc is interpreted as the effects of shallow magma chambers. The doubling of the crust in the back-arc region affects the lithospheric thermal structure considerably, but models do not show reverse temperature–depth distributions in the continental crust. In the back-arc region the transition from a thermally thinned lithosphere to a 'normal' lithospheric thickness for continental shields may occur. The observed surface heat-flow density in the Andean foreland suggests lithospheric thermal conditions as typical for shield areas. © 1999 Elsevier Science B.V. All rights reserved.

Keywords: heat-flow density; central Andes; numerical modelling; lithospheric thermal regime; subduction; crustal doubling

[*] Fax: +49 331 2881450; E-mail: springer@gfz-potsdam.de

1. Introduction

The lithospheric thermal structure of convergence zones is not well known, but is a key factor in order to understand tectonic processes which are related to the active subduction process, as these processes are controlled by physical properties which critically depend on temperature. The surface heat-flow density can be used to constrain quantitative models of the lithospheric thermal field in relation to different tectonic scenarios and parameter variations. In general, most subduction zones show similar characteristic heat-flow density patterns. The more regional heat-flow density pattern may be superimposed by local, near-surface effects such as, for example, the cooling of magma chambers at shallow depth. Quantitative models of different processes that influence the thermal structure and thus the heat-flow density can be used to distinguish between lithospheric processes and local near-surface effects and therefore could provide important clues to understand these tectonic processes.

The South American Andes present the type example of an active continental margin where the oceanic Nazca plate subducts beneath the South American continent. In the past four decades, heat-flow density determinations in the central Andes and the Nazca plate were the focus of several studies (Von Herzen, 1959; Sclater et al., 1970; Uyeda and Watanabe, 1970, 1982; Anderson et al., 1976; Uyeda et al., 1978, 1980; Watanabe et al., 1980; Henry, 1981; Muñoz, 1987; Henry and Pollack, 1988; Muñoz and Hamza, 1993; Kudrass et al., 1995; Springer, 1997; Springer and Förster, 1998). From this work heat-flow density maps were derived to examine the variation of the geothermal regime related to different tectonic settings. One-dimensional analytical estimates have been used to interpret the central Andean surface heat-flow density pattern (Giese, 1994; Favetto et al., 1997). These models do not include effects related to the subduction process, such as underthrusting of the cold oceanic lithosphere, frictional heat generation along the plate contact or mantle flow induced by the subducting slab. Several authors have studied the thermal structure of different subduction zones using numerical models (e.g. Toksöz et al., 1971; Andrews and Sleep, 1974; Van den Beukel and Wortel, 1988;

Dumitru, 1991; Davies and Stevenson, 1992; Furukawa, 1993; Peacock, 1993; Hyndman and Wang, 1993, 1995) or analytical calculations (e.g. Molnar and England, 1990, 1995; Tichelaar and Ruff, 1993a). These models show large differences in lithospheric temperatures which are mainly caused by different model inputs, such as the model geometry, petrophysical parameters, and effects linked with the subduction process itself.

The objective of this paper is the interpretation of the surface heat-flow density pattern in the central Andes with regard to ongoing tectonic processes. Different scenarios of the prevailing tectonic processes and the variation of geometrical and petrophysical parameters are simulated using numerical models to analyse the lithospheric thermal field. Their influence on the lithospheric thermal field is demonstrated and heat-flow components attributed to lithospheric processes are separated from near-surface effects. Because of the sparse information on the lithospheric structure and petrophysical parameters in the central Andes, the models are kept simple and focus on the investigation of principal effects.

2. Tectonic setting

The central Andes provide a present-day example of an ocean–continent subduction zone. In northern Chile the subduction of the oceanic Nazca plate beneath the continental South American plate is ongoing since about 200 Ma (Coira et al., 1982). The age of the oceanic Nazca plate along the subduction zone is older in the north and younger in the south. At 21ºS the age of the subducting plate is about 50 Ma (Cande and Haxby, 1991; Müller et al., 1997). The Nazca–South American plate convergence velocity is 84 mm a^{-1} (DeMets et al., 1990). The Wadati–Benioff zone can be traced to more than 600 km deep (Cahill and Isacks, 1992; Kirby et al., 1995). The dip angle varies with depth from less than 10º at 0 to 20 km depth, 15–17º at 20 to 60 km depth, 20–26º at 60 to 100 km depth, 25–32º at 100 to 150 km depth and steepens to greater than 33º for depths >150 km (Comte and Suárez, 1995). The maximum depth of seismic coupling in northern Chile extends to about 45–50 km depth (Tichelaar and Ruff, 1991, 1993b; Suárez and Comte, 1993). The present topography

of the central Andes has mainly developed since the Late Oligocene (Jordan and Gardeweg, 1989). The Altiplano–Puna plateau has an average elevation near 4000 m extending over an area of about 1500 km long (N–S) and 300 km wide (E–W). The minimum in the Bouguer anomaly of about −450 mGal (Götze and Kirchner, 1996) and teleseismic investigations (Zandt et al., 1994; Beck et al., 1996) indicate a thickened Andean crust of about 65–75 km. The lateral extent of the thickened crust correlates remarkably with the region of high topographic elevation. The western border of the plateau is the recent magmatic arc. The fore-arc region is formed by older magmatic arc systems, which migrated stepwise from the west to the east (Coira et al., 1982; Scheuber et al., 1994). The Coastal Cordillera represents the oldest magmatic arc formed during Jurassic time. In the Early Cretaceous, the magmatic activity shifted eastward to the present Longitudinal Valley. The third magmatic arc has been located in the Precordillera which developed during Late Cretaceous to Palaeogene time. Since the Miocene magmatic activity has been located within the Western Cordillera and partly in the Altiplano region.

The eastern edge of the Altiplano–Puna plateau is formed by the Eastern Cordillera, characterised by west- and east-verging thrusts. Adjacent to the east, the east-verging fold-and-thrust belt of the Subandean Ranges represents the eastern flank of the central Andes. The foreland of the Subandean Ranges is formed by the sedimentary basin of the Chaco, which is part of the stable Brazilian Shield.

The thickened Andean crustal structure has been explained by various processes (see e.g. recent discussion in Allmendinger et al., 1997): underplating of the Brazilian Shield under the Andean crust (Roeder, 1988; Schmitz, 1994; Lamb et al., 1997), magmatic addition (Thorpe et al., 1981) and thermal uplift in combination with crustal shortening (Isacks, 1988). Crustal thickening in the region of the Eastern Cordillera can be explained by tectonic shortening, while in the Altiplano and the fore-arc region other processes may dominate (Schmitz, 1994; Schmitz and Kley, 1997). Crustal thickening of the central Andes is interpreted to be developed in two major stages (e.g. Gubbels et al., 1993; Jordan et al., 1997; Okaya et al., 1997). In the first stage, beginning in the Late Oligocene, crustal shorten-

ing was located mainly in the plateau region and Eastern Cordillera. The total amount of crustal shortening for the Altiplano and Eastern Cordillera is not well known; estimates vary from 100-155 km (Isacks, 1988; Schmitz, 1994) up to about 250 km (Lamb et al., 1997). However, a significant portion of crustal volume in the plateau region (10–30%) must be explained by other processes as, for example, magmatic addition, tectonic underplating or hydration processes of upper mantle rocks. Geophysical investigations of the crust beneath the Altiplano and Western Cordillera show low seismic velocities, which are explained either by a felsic composition of the lower crust (Zandt et al., 1994), or large amounts of partially molten rocks (Schmitz et al., 1997). Parts of the deeper fore-arc crust are discussed as underplating of tectonically eroded material from the continental margin (Schmitz, 1994). In the second stage, widespread crustal shortening began on the eastern side of the Andean mountain belt (thrust belt of the Subandean zone) in the Late Miocene (about 10 Ma). During this phase, the entire crust of the Subandes was thrust westward beneath the Eastern Cordillera. Crustal shortening of about 140–150 km, accumulated since the Miocene, has been estimated for the area of the foreland to the Eastern Cordillera (Gubbels et al., 1993; Schmitz, 1994; Schmitz and Kley, 1997).

3. Heat-flow density in the Central Andes

Compilations of available heat-flow density data between the Nazca plate adjacent to the Andean subduction zone and the Chaco basin are reported in several recent studies (e.g. Henry and Pollack, 1988; Hamza and Muñoz, 1996; Springer and Förster, 1998). The regional distribution and quality of the primary geothermal data used for heat-flow density determinations in the central Andes are extremely variable. A total of 74 reliable heat-flow density data (Springer, 1997; Springer and Förster, 1998) could be obtained for the study area (between 15–30ºS and 60–75ºW). About one third of the data set, located in the Subandean Ranges and the Chaco basin, is derived from bottom-hole temperatures. 16% of the heat-flow sites are situated within the Eastern Cordillera, where heat-flow density determinations

are mainly based on temperature measurements in underground mines. Heat-flow density determinations in the fore-arc region, the active magmatic arc and the Altiplano plateau (about 40% of the data set) are predominantly derived from continuous temperature logs in boreholes. Temperature readings within the area of the oceanic Nazca plate (about 10% of the data set) and within Lake Titicaca are obtained at shallow depths in unconsolidated sediments. Due to the inhomogeneity in the data quality and distribution, only general trends of heat-flow density related to tectono-morphologic units can be derived. The most important features of the heat-flow density pattern as described by Springer and Förster (1998) are as follows. Along strike of the Andean orogen (N–S) no significant changes are found, but there are major variations across the orogen (W–E). The heat-flow density of the Nazca plate decreases with increasing distance from the East Pacific Rise from higher than 100 mW m^{-2} to about 40 mW m^{-2} near the central Andean subduction zone (see also heat-flow density map of Pollack et al., 1993). In the region of the Peru–Chile trench heat-flow density is about 30 mW m^{-2}. Heat-flow density in the Coastal Cordillera is on an average of 20 mW m^{-2} and presents a heat-flow minimum. Towards the east, in the fore-arc region (Longitudinal Valley and Precordillera), heat-flow density increases to values between 40 and 60 mW m^{-2}. The data base from the active magmatic arc (Western Cordillera) and the adjacent high plateau of the Altiplano is extremely sparse. The heat-flow density pattern is characterised by large variations from 50 to 180 mW m^{-2}. A comparatively high heat-flow density of about 80 mW m^{-2} is also characteristic of the back-arc region immediately to the east (Eastern Cordillera). Towards the Subandean Ranges and Andean foreland (Chaco basin), heat-flow density decreases to about 40 mW m^{-2}.

4. Thermal models

The main tectonic processes and their effects on the lithospheric thermal field are analysed by forward modelling along a profile across the central Andes at about 21ºS. Three different types of models are applied (Fig. 1): the fore-arc region between the trench and the active magmatic arc is analysed by 2-D sub-

duction models; the back-arc region, which is characterised by crustal doubling is investigated using 2-D crustal stacking models describing simple underthrust phenomena; and for the region of the Andean foreland, which reflects stable shield conditions, 1-D temperature estimates are applied. Surface heat-flow density is used to constrain the thermal models with various geometrical parameters (e.g. subduction angle and velocity) and petrophysical parameters (e.g. thermal conductivity, radiogenic and frictional heat generation). To solve the heat conduction equation for a 2-D space, a standard finite-element method with a Galerkin formulation is applied.

4.1. 2-D subduction model

4.1.1. Model parameters

The subduction model comprises two different parts, the subducting oceanic Nazca plate and the fixed South American continental lithosphere, that do not deform with time. The subduction angle (α) and the velocity (v) of the subducting plate are constant with time. An oceanic lithosphere of 100 km thickness with a 10 km thick crust (Wigger et al., 1994) is considered. Assuming a mean subduction angle α of 20º (Comte and Suárez, 1995) and a constant distance between the trench and the volcanic line of 260 km (distance C–A in Fig. 1), the top of the subducting slab below the volcanic line is reached at 95 km depth (point F in Fig. 1). Below the volcanic line a crustal thickness of 70 km is assumed; the maximum depth of the contact between the continental and oceanic crust (point D in Fig. 1) is fixed at 60 km (Schmitz, 1994). The region between the continental crust and the subducting slab is treated in two different ways. A reference model considers a lithospheric mantle, which implies a pure conductive heat transport. To investigate the impact of an asthenospheric mantle wedge on crustal temperatures and the surface heat-flow density, an isothermal boundary condition (1250ºC) is assumed below the continental crust (further details later in the text).

The following boundary conditions are used (see Fig. 1). (1) A fixed surface temperature of 0ºC is assumed. (2) The pre-subduction geotherm is approximated by a steady-state geotherm of an oceanic lithosphere corresponding to a surface heat-flow den-
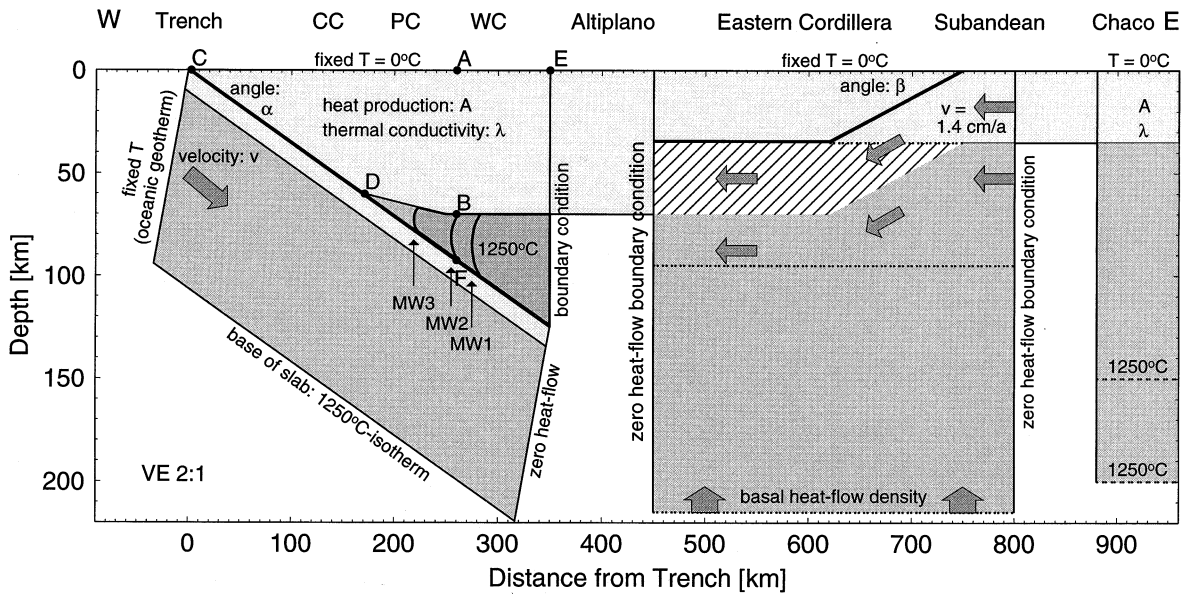
Fig. 1. Geometries and boundary conditions of the three different numerical models along the W–E profile: (1) the subduction model in the west, (2) the crustal stacking model in the central part of the profile and (3) the 1-D geotherm model in the east. *MW1–3* represent models assuming different westward extent of an asthenospheric mantle wedge in contrast to the reference model (RFM) which assumes a lithospheric mantle wedge (conducting lithosphere without 1250°C-isotherm within the wedge). Physical parameters and their variations are explained in Tables 1 and 2; *CC* is Coastal Cordillera; *PC* is Precordillera; *WC* is Western Cordillera.

sity of 40 mW m^{-2} (Springer and Förster, 1998). (3) A temperature of 1250°C is assumed at the base of the subducting slab. (4) A zero vertical heat-flow boundary condition is used at the right hand side of the model. Material parameters used in thermal modelling are summarised in Table 1.

An automatic mesh-generation procedure was applied to the model configuration. A close finite-element grid spacing along the zone of plate contact of 2 km and a coarser grid spacing of 5 km for the other parts of the model is found to be appropriate. This procedure enables the transition of a high mesh density in regions that are influenced

to a great extent by the subduction process to a coarser mesh density in regions that are less affected by the subduction process. The study neglects transient effects and solves for the steady-state solution. Thermal models of subduction zones presented by Van den Beukel and Wortel (1988) show nearly steady-state conditions at 30 Ma after the initiation of subduction and a completely steady-state thermal structure at about 50 Ma. The subduction process of the central Andes has continued since about 200 Ma, which substantiates the assumption of steady-state conditions. However, an essential condition for this assumption are constant subduction variables for

Table 1
Physical parameters used in thermal modelling

Layer	Density (kg m^{-3})	Thermal conductivity (W mK^{-1})	Thermal diffusivity (m^2 s^{-1})	Specific heat (J kg^{-1} °C^{-1})	Radiogenic heat production (μW m^{-3})
Continental crust	2700	2.5	10^{-6}	1000	0.90
Oceanic crust	2700	2.5	10^{-6}	1000	0.25
Lithospheric mantle	3300	3.3	10^{-6}	1000	0.02

Parameters correspond to a reference model; variations of particular parameters are described in the text and are summarised in Table 2.

that period of time. Some subduction parameters in the central Andes vary considerably with time (e.g. subduction velocity; Pardo-Casas and Molnar, 1987). Investigations of their influence on the thermal structure will improve our understanding of whether or not steady-state calculations provide useful results.

To investigate the influence of different parameters on the lithospheric thermal field, variations of the following parameters are considered (summarised in Table 2): (1) the subduction angle; (2) the subduction velocity; (3) the shear stress distribution along the plate contact; (4) the westward extent of an asthenospheric mantle wedge; (5) the crustal radiogenic heat production; and (6) the temperature-dependence of the thermal conductivity.

In order to keep the model simple, the increase in dip with increasing depth of the subducting slab, as observed by Comte and Suárez (1995), is neglected. The constant dip angle (α) is varied from 10 to 30º to investigate its impact on crustal temperatures.

The convergence rate between the Nazca and the South American plates has varied since the latest Cretaceous from less than 5 cm a^{-1} to more than 10 cm a^{-1} (Pardo-Casas and Molnar, 1987). Therefore, variations of the subduction velocity (v) from 1 to 12 cm a^{-1} were made to investigate the influence of this parameter on the crustal thermal field.

A key parameter for the lithospheric thermal field is the amount of frictional heating on the slip surface of the two lithospheric plates. The amount of

Table 2
Varying parameters for the different types of thermal models

Model		Parameter variation
2D-subduction model	1.	Subduction angle (α): 10–30º
	2.	Subduction velocity (v): 1–12 cm a^{-1}
	3.	Frictional heat generation at plate contact
		RFM: constant shear stress (15 MPa)
		SH1: zero shear stress
		SH2: linear increase $\leq$40 km, constant >40 km depth
		SH3: linear increase $\leq$40 km, exp. decrease >40 km depth
	4.	Asthenospheric mantle wedge
		MW1: max. westward extent east of the volcanic line
		MW2: max. westward extent below the volcanic line
		MW3: max. westward extent west of the volcanic line
	5.	Crustal radiogenic heat generation
		a: $A(z) =$ constant $= 0.9$ μW m^{-3}
		b: $A(z) = A_0 \exp(-z/D)$, $A_0 = 1.5, 3.0, 4.0$ μW m^{-3}
	6.	Thermal conductivity
		a: constant (see Table 1)
		b: temperature-dependent ($\lambda = \lambda_0/(1 + cT)$)
Isolated magma chambers	1.	Depth of magma chamber
2D-crustal stacking model	1.	Basal heat-flow density
		a: initial conditions correspond to the Eastern Cordillera
		b: initial conditions correspond to the Subandean
	2.	Shear stress along the thrust
		a: low shear stress (10 MPa)
		b: high shear stress (100 MPa)
1D-geotherm model	1.	Lithospheric thickness: 150 or 200 km
	2.	Crustal radiogenic heat generation
		a: $A(z) =$ constant $= 0.9$ μW m^{-3}
		b: $A(z) = A_0 \exp(-z/D)$, $A_0 = 1.5, 3.0$ μW m^{-3}
	3.	Thermal conductivity:
		temperature-dependent ($\lambda = \lambda_0/(1 + cT)$)

For the modelling only a single parameter is varied, all other parameters correspond to the reference model given in Table 1.

frictional heat produced per unit area of plate contact equals the product of shear stress and subduction velocity. For brittle deformation the average shear stress increases linearly with the effective normal stress (normal stress minus pore-fluid pressure; Turcotte and Schubert, 1982). Pore-fluid pressures play a prominent role within subduction zones and can be very close to lithostatic pressures resulting in only low effective shear stresses. Flow laws for ductile deformation by steady-state dislocation creep are generally expressed by a power law (Kirby, 1983). For the estimation of the shear stress in a ductile deformation regime, the knowledge of several material parameters is essential. Some of these parameters, such as pore-fluid pressure, strain rates and material constants are poorly constrained. Thus, a given amount of shear stress along the plate contact is assumed. Following the estimates of Froidevaux and Isacks (1984) and Tichelaar and Ruff (1993a) a mean shear stress of 15 MPa along the plate contact is used down to 125 km depth. For the finite-element modelling a volumetric form of the frictional heat production is needed, which can be implemented by dividing the amount of frictional heat generation by the channel width. A channel width of 1 km is assumed; the channel width has a negligible influence on equilibrium temperatures (Yuen et al., 1978).

The distribution of shear stress with depth has been varied in the following way (see Fig. 2): a constant shear stress of 15 MPa has been assumed over the entire depth range (Reference Model, RFM), SH1 a zero shear stress, SH2 a linear increase up to 40 km depth and a constant value for greater depths, and SH3 a linear increase of shear stress up to 40 km depth and an exponential decrease for greater depths. The summed mean shear stress over the entire depth range of both SH2 and SH3 is 15 MPa.

After Isacks (1988), the uplift of the Altiplano–Puna plateau is attributed to thickening of a ductile lower crust by compressional tectonics and thermal lithospheric thinning. As a first-order approximation for thermal modelling this process can be described by an isotherm corresponding to the lithosphere/asthenosphere boundary at shallow depth. Therefore, a 1250ºC-isotherm is assumed at shallow depth and its westward extent into the wedge is varied. Three different cases are investigated (see Fig. 1): MW1 the maximum extent of the
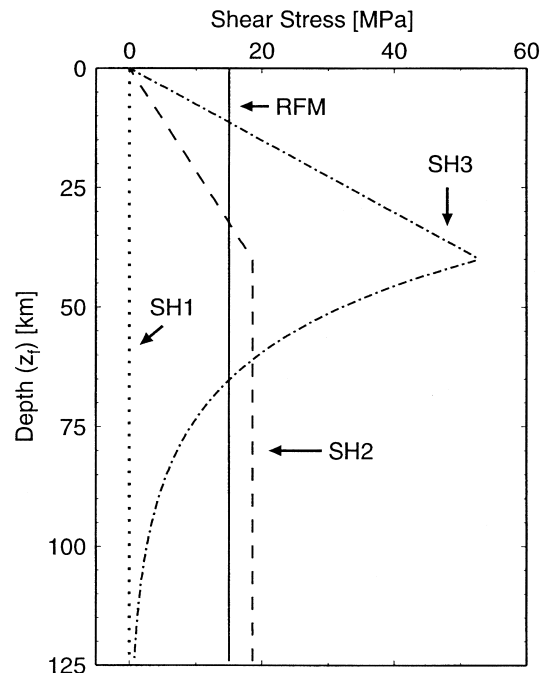

Fig. 2. Assumed shear stress distributions along the plate contact (profile C–D in Fig. 1). Constant shear stress of 15 MPa over the entire depth range (Reference model (*RFM*), solid line): *SH1*, dotted line, zero shear stress; *SH2*, dashed line, linear increase up to 40 km depth and a constant value for greater depths; *SH3*, dashed/dotted line, linear increase of shear stress up to 40 km depth and an exponential decrease for greater depths. Summed mean shear stress over the entire depth range in both SH2 and SH3 is 15 MPa.

1250ºC-isotherm into the wedge is located east of the volcanic line, MW2 below the volcanic line, and MW3 west of the volcanic line.

Radiogenic heat production in the oceanic and the continental plate is assumed to be constant for most models (see Table 1). Additional models consider a depth-dependent radiogenic heat production for the continental crust given by $A(z) = A_0 \exp(-z/D)$, where A_0 is the radiogenic heat-production rate at the Earth's surface, z is depth, and D is the radiogenic scaling depth. A radiogenic scaling depth of 10 km (Čermák and Haenel, 1988) for the whole crust and surface radiogenic heat-production rates of 1.5, 3.0 and 4.0 $\mu W\ m^{-3}$ are assumed. Crustal heat production decreases with depth to a minimum value of 0.45 $\mu W\ m^{-3}$ for lower crustal rocks (Chapman and Furlong, 1992); for greater depths heat production is set at this value.

In thermal models investigating the entire lithospheric thickness, the temperature dependency of thermal conductivity has to be taken into account. Experimental data show a decrease of the thermal conductivity of more than 50% with an increase in temperature from 0 to 1000ºC (Zoth and Haenel, 1988; Clauser and Huenges, 1995). Thermal conductivity of the reference model is assumed to be constant (see Table 1). Additional calculations consider a thermal conductivity dependency given by $\lambda = \lambda_0/(1+cT)$ (Čermák and Rybach, 1982), where λ_0 is the thermal conductivity at 0ºC and c is a material constant (assumed as $10^{-3}ºC^{-1}$). Following the compilations from Zoth and Haenel (1988), thermal conductivity values at surface conditions (λ_0) have been set to 3.0 W m^{-1} K^{-1} for crustal rocks and 4.4 W m^{-1} K^{-1} for subcrustal rocks.

4.1.2. Model results

The general steady-state fore-arc thermal structure is characterised by downward-deflected isotherms caused by the subduction of cold oceanic lithosphere. Wider isotherm spacing results in low geothermal gradients and a pronounced minimum in the surface heat-flow density (see Fig. 3c and Fig. 6). In the region of the volcanic arc the crustal temperature structure is less affected by the subduction process and the isotherms become subhorizontal. Lithospheric cooling by the subduction of the oceanic plate on the one hand and frictional heating along the plate contact on the other hand can result in reverse temperature–depth functions in the fore-arc region. Deeper parts of the oceanic lithosphere are not influenced by frictional heating along the slip surface.

In the reference model the subduction angle is set to a constant value of 20º. Resulting crustal temperatures and the heat-flow density distribution across the subduction zone are shown in Fig. 3. Variation of the dip angle between 10 and 20º has only moderate impact on crustal temperatures in the fore-arc region. Compared to the reference model, differences in temperature of a maximum of +90ºC at 60 km depth are calculated for shallow subduction with a dip angle of 10º. The effect on the surface heat-flow density is less than 10 mW m^{-2}. More significant is the effect on the lateral extent of the resulting heat-flow density minimum. Steeper subduction results in

a narrow heat-flow density minimum, in contrast to a very distinct heat-flow density minimum caused by shallow subduction angles.

The effect of subduction velocity on the thermal structure turns out to be very small (see also Van den Beukel and Wortel, 1988). Variations of subduction velocity between 6 and 12 cm a^{-1} do not result in significant differences in the thermal structure compared to the reference model ($v = 8.4$ cm a^{-1}). The effects of increased cooling caused by faster subduction and the higher heat production by friction cancel each other out (Van den Beukel and Wortel, 1988). In the case of very slow subduction ($v = 1$–3 cm a^{-1}), the effect of heating of the oceanic lithosphere by the hotter overlying continental crust exceeds the effect of cooling, and along the plate contact at 60 km depth the resulting temperatures are about 150ºC higher than in the reference model.

Shear stress and the resulting frictional heating along the plate contact has the most important influence on the thermal structure of the fore-arc. Most of the generated frictional heat is consumed to heat up the downgoing slab (see Van den Beukel and Wortel, 1988). The influence on temperatures of the overlying plate is significant in the fore-arc close to the trench but tends to be negligible towards the volcanic arc (Fig. 3b,d). The variation of the shear stress distribution along the plate contact results in temperature variations from less than 200ºC to more than 400ºC at the maximum depth of the plate contact (60 km). The resulting heat-flow density distributions show noticeable changes only in the fore-arc region between the trench and the Coastal Cordillera; towards the volcanic line the surface heat-flow density tends toward a value of about 50 mW m^{-2}. Observed heat-flow density conditions in the region of the Coastal Cordillera (about 20 mW m^{-2}) are met when an extremely low shear stress at shallow depth is assumed. Shear stress distributions at greater depths cannot be distinguished from the surface heat-flow density.

Petrological studies of volcanic centres within the Central Volcanic Zone (CVZ, see summary by Francis and Hawkesworth, 1994) show mainly mantle-derived basaltic magma compositions. Therefore, temperature conditions in the mantle wedge below the active volcanic arc must exceed melting conditions of mantle rocks. To generate such conditions at
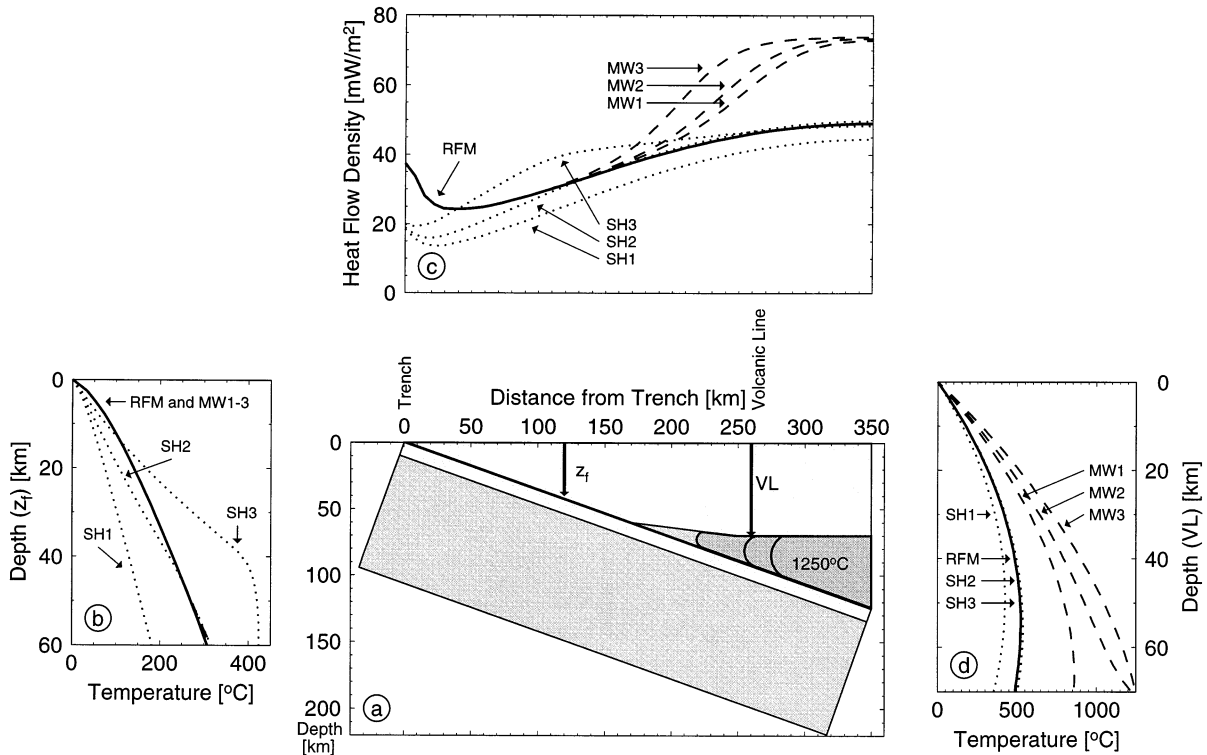
Fig. 3. (a) Geometry of the 2D-subduction model. (b) Resulting temperatures along the plate contact versus depth z_f (along profile C–D in Fig. 1). (c) Resulting surface heat-flow density (profile C–E in Fig. 1). (d) Resulting crustal temperatures below the volcanic arc (profile A–B in Fig. 1). Models: *RFM*, solid line = reference model with parameters of Table 1; *SH*, dotted lines = models assuming different shear stress distributions along the plate contact (see Fig. 2); *MW*, dashed lines = models assuming different westward extent of an asthenospheric mantle wedge (see Fig. 1).

subcrustal levels by shear heating, shear stresses in excess of 100 MPa are required. Such shear stresses are 1–2 orders of magnitude higher than estimates of rock strength at elevated pressures and temperatures (see Yuen et al., 1978; Peacock, 1989). Furthermore, frictional heating decreases drastically at temperatures higher than those of the brittle–ductile transition and thus cannot explain melting temperatures below the volcanic arc. Therefore, other scenarios such as the occurrence of an asthenospheric mantle wedge at shallow depth have to be assumed. An asthenospheric mantle wedge implies advective heat transport of hot material, which can be more effective than conductive cooling caused by the subduction of cold oceanic lithosphere. Numerical models considering mantle flow induced by the subducting slab (e.g. Davies and Stevenson, 1992; Furukawa, 1993) show a similar pattern of the stream lines

and the calculated isotherms in the mantle wedge as simplified in this study. The influence of the westward extent of the 1250°C-isotherm into the wedge is shown in Fig. 3. In contrast to the volcanic arc region, temperatures in the fore-arc close to the trench are not influenced by the asthenospheric mantle wedge. Calculated heat-flow density profiles show a general increase to the volcanic arc, but the effect on the surface heat-flow density is too small to be distinguished by the measured heat-flow density profile. However, to match conditions for melting at subcrustal levels in the volcanic arc region, the minimum extent of the 1250°C-isotherm has to coincide with the position of the volcanic arc. Otherwise, the cooling effect of the subduction process results in too low temperatures at subcrustal levels. Because of the boundary conditions $T_s = 0°C$ and $T_{asth.} = 1250°C$ used for the modelling, only general statements on

the thermal structure of the continental crust can be made. The maximum heat-flow density in the region of the volcanic arc is on the order of 60–70 mW m^{-2}. Locally higher values in the volcanic arc have to be interpreted by near-surface effects, such as shallow isolated magma chambers (see later in the text).

The variation of the radiogenic heat-production rate affects the near-surface thermal field considerably, but the temperatures at greater depths are only slightly affected. This is a consequence of the assumed accumulation of radioactive elements in the upper crust, its exponential decrease with depth, and the increase of crustal thickness towards the volcanic arc. Model calculations with a high radiogenic heat-production rate at the surface (4.0 μW m^{-3}) show an almost constant heat-flow density across the subduction zone of about 40 mW m^{-2}. The high heat production in the fore-arc cancels out the low surface heat-flow density caused by the advection of cold material. Model calculations with lower surface radiogenic heat-production rates show similar heat-flow density profiles respectively at lower levels.

Additional calculations were done considering temperature-dependent thermal conductivities. Model calculations assuming constant average thermal conductivities (see Table 1) yield almost the same results as models with temperature-dependent conductivities, which implies a good approximation of the average values with the assumed temperature dependency.

4.1.3. Isolated magma chambers

The influence of isolated magma chambers on the surface heat-flow density can be estimated by analytical solutions (Carslaw and Jaeger, 1959; Haenel and Mongelli, 1988). To analyse their impact on the surface heat-flow density pattern during the cooling process, an intrusive body is approximated by a rectangular parallelepiped. The estimation of an 'average' magma chamber volume is extremely complicated. Published ratios of extrusive to intrusive rocks are on the order of 1 : 1 to 10 : 1, and only rarely can magma chamber volumes be estimated. However, these ratios may strongly differ according to the magma composition and are variable for different volcanoes. In the following, a magma chamber with an extent of 7 × 7 × 4 km (length × width × height) and an initial magma chamber temperature

of 1000ºC, appropriate for andesitic magma, will be assumed.

The impact of an isolated magma chamber on the surface heat-flow density is mainly influenced by its depth. The deeper the magma chamber, the smaller the surface effect. A magma chamber at 4–8 km depth results in a relative heat-flow density anomaly on the order of 150 mW m^{-2}. The anomaly can be recognised only within a relatively small time span. About 1 Ma after the onset of cooling the anomaly diminishes to about 10 mW m^{-2}. The same magma chamber, located just 1 km deeper at 5–9 km depth, results in a heat-flow density anomaly on the order of 90 mW m^{-2}. Assuming an intrusion depth below 10 km, the resulting heat-flow density anomaly is on the order of 10 mW m^{-2} and cannot be resolved in the case of the central Andean heat-flow data set. The width of the surface heat-flow density anomaly (of magnitude greater than 10 mW m^{-2}) is about twice the magma chamber width.

4.2. 2-D crustal stacking model

4.2.1. Model parameters

In order to investigate the thermal evolution during the process of underthrusting in the back-arc region, a 2-D crustal stacking model is used (see Fig. 1). In contrast to the long-lasting subduction process (since about 200 Ma), strong shortening in the back-arc region started in the Late Miocene. For this rather recent process steady-state conditions cannot be assumed (Shi and Wang, 1987; Peacock, 1989). Transient phenomena caused by, for example, heat advection (emplacement) and simultaneous temperature relaxation have to be considered. The initial temperature condition (at $t = 0$) for the crustal stacking model is represented by a horizontal homogeneous temperature field corresponding to a 35 km thick crust underlain by a lithospheric mantle. The underthrusting of the entire lithosphere relative to the fixed upper crustal segment is modelled in two steps. (1) For technical reasons, the replacement of lithospheric mantle material by underthrusted crustal material is instantaneous (shaded area in Fig. 1). (2) Afterwards, a constant velocity is assigned to the entire underthrusting lithosphere. The thicknesses of the two crustal segments remain unchanged during underthrusting, resulting in a doubled crust of 70

km thickness. Processes like tectonic uplift, erosion and isostatic uplift are not considered in the model. Isostatic compensation has only modest influence to the lithospheric thermal field (Germann, 1990); in contrast erosion may have significant effects on the thermal state of the upper crust, which will be discussed separately below.

The following boundary conditions are used (Fig. 1): (1) A fixed surface temperature of 0ºC is assumed. (2) A zero horizontal heat-flow boundary condition ($\partial T/\partial x = 0$) at the right hand side and left hand side of the model is used. (3) At the lower boundary of the model a variable basal heat-flow density is applied. Following the estimates for the total amount of crustal shortening of about 140 km since the Miocene (Gubbels et al., 1993; Schmitz, 1994; Schmitz and Kley, 1997), a constant relative velocity for underthrusting of 1.4 cm a^{-1} for a period of 10 Ma is assumed. The lithosphere is thrusting under the fixed crustal segment at an angle of 15º (Schmitz, 1994). All petrophysical parameters correspond to the values of Table 1.

This simplification of the crustal stacking process results in models where crustal parameters within the zone of the thickened crust are used for the entire period of time instead of a progressive displacement of crustal material. To verify the error of temperature estimates based on this simplification, a calculation simulating a duration of 10 Ma is made considering an instantaneous replacement of lithospheric mantle material by underthrusted crustal material, but without any velocity assignment to the underthrusted lithosphere. Because of the different petrophysical parameters, temperatures within the underthrusted lithosphere are a maximum of 65ºC higher than initial temperatures. This range is considered to be the error of temperature estimates based on the simplification of the crustal stacking process.

Two different scenarios are investigated by varying the basal heat-flow density. In the first case, a basal heat-flow density of 12 mW m^{-2} is applied, to approximate initial surface conditions corresponding to the surface heat-flow density in the Subandean Ranges. Resulting initial conditions of surface heat-flow density are approximately 45 mW m^{-2} and the lithosphere/asthenosphere boundary is at about 200 km depth. In a second case, corresponding to the surface conditions of the Eastern Cordillera, a basal heat-flow density of 30 mW m^{-2} is applied, resulting in a surface heat-flow density of about 60 mW m^{-2} and a lithospheric thickness of about 100 km (see Fig. 1 and right-hand side of thermal structures of Fig. 4). Again, as in the 2D-subduction models, shear stress is considered in the 2D-crustal stacking model. Along a 1-km-thick thrust, the amount of shear stress is variable. For both initial conditions a low friction model with a constant shear stress of 10 MPa and a high friction model with a shear stress of 100 MPa is investigated.

4.2.2. Model results

Fig. 4 shows the resulting thermal structures and surface heat-flow density distributions for various parameters of the crustal stacking model 10 Ma after the onset of thrusting. Initial conditions can be seen on the right side of the models; the advective heat transport in lateral direction does not affect the thermal field. The general thermal structure is similar to the subduction models, showing downward deflected isotherms caused by underthrusting. The wider isotherm spacing results in low geothermal gradients and a surface heat-flow density minimum. The low shear stress models (Fig. 4a,b) yield a surface heat-flow density minimum of about 20 mW m^{-2}. There is no increase in the surface heat-flow density caused by the thickened crust and corresponding greater radiogenic heat production. This effect results in a significant increase of the surface heat-flow density only after longer times (about 50 Ma). Reverse temperature–depth distributions in the crust, as usually assumed in one-dimensional models for temperature relaxation of an initial 'sawtooth' geotherm (see discussion in Peacock, 1989), do not result from the 2-D crustal stacking models. In contrast, reverse temperature–depth functions result in the case of high shear stress along the thrust (Fig. 4a′,b′). The frictional heat generation within the 1 km thick thrust is about 50 times higher than the radioactive heat generation of the surrounding crustal material, resulting in higher temperatures close to the thrust. The effect of crustal cooling by underthrusting is diminished by the high frictional heating and a pronounced minimum in the surface heat-flow density cannot be resolved. Assuming melting conditions in the lower crust as a maximum temperature limit, and further that the composition of the lower
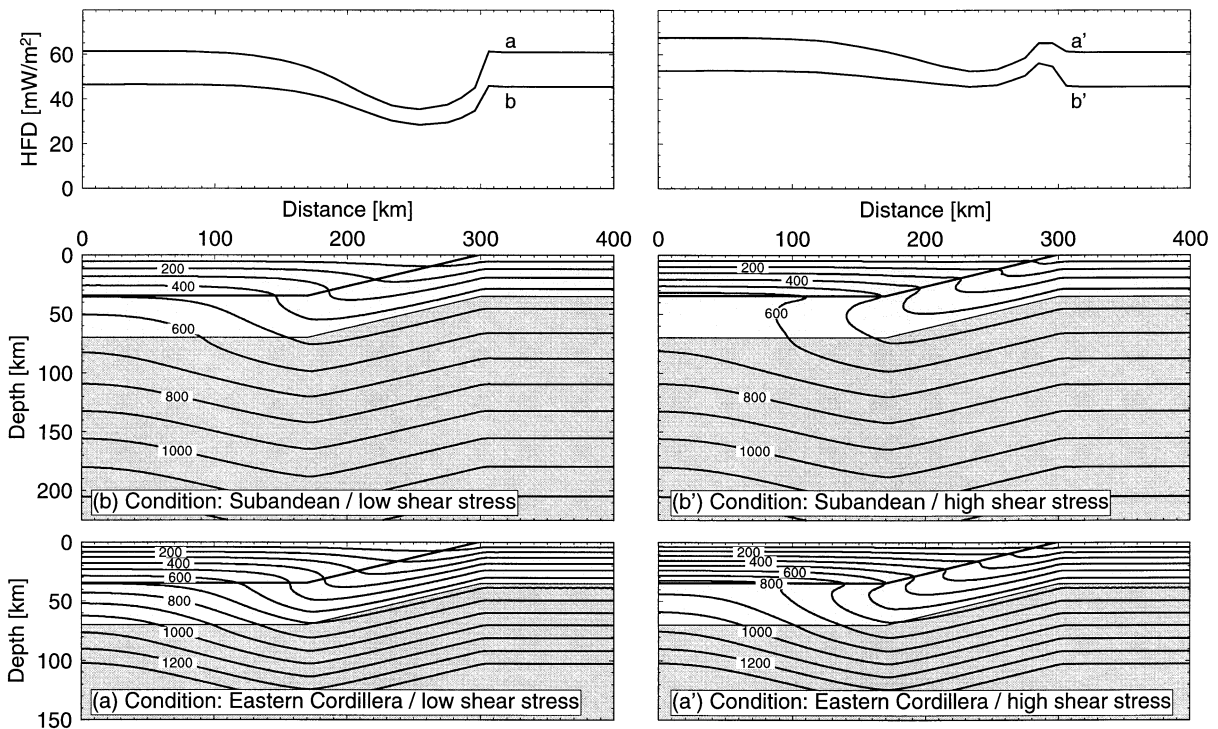
Fig. 4. Geometry of the crustal stacking model and thermal structures 10 Ma after the onset of thrusting. (a, a′) Initial conditions correspond to the conditions of the Eastern Cordillera with a surface heat-flow density of 60 mW m^{-2} and a lithospheric thickness of about 100 km. (b, b′) Initial conditions correspond to the conditions of the Subandean Ranges with a surface heat-flow density of 45 mW m^{-2} and a lithospheric thickness of about 200 km. Models assume a constant shear stress along the thrust of 10 MPa (a and b) or 100 MPa (a′ and b′). Thermal field is shown in contour intervals of 100ºC.

crust corresponds to that of tholeiitic basalt (melting temperatures on the order of 1000ºC), a maximum surface heat-flow density on the order of 60 mW m^{-2} is calculated at the left side of the model.

The development of the major topographic relief of the Eastern Cordillera occurred within the last 10 Ma (Gubbels et al., 1993; Okaya et al., 1997). This uplifted region has since been subject to erosion. The effect of erosion on uppermost crustal temperature conditions is to expose warmer rocks, which contributes to an increase in temperature gradient and thus surface heat-flow density. Erosional processes are not considered in the numerical models. The perturbation of the thermal field by erosion can be described analytically by heat conduction in a moving medium (Carslaw and Jaeger, 1959, p. 388). Published erosion rates of 0.2–0.4 mm a^{-1} in the last 10–15 Ma (Crough, 1983) will increase the heat-flow density at the surface by about 10–30%.

4.3. 1-D geotherm model

4.3.1. Model parameters

The Andean foreland is characterised by large sedimentary basins, such as the Chaco basin, underlain by the Precambrian Brazilian Shield. The geothermal regime of such shields is mainly influenced by the heat that flows upward from the mantle and by internal crustal heat sources. Effects on the thermal structure in the sedimentary basin such as heat advection through extensive aquifers are neglected. Thus one-dimensional, steady-state conditions are assumed for the lithospheric thermal regime of the Andean foreland. Boundary conditions for the calculations are a fixed surface temperature of 0ºC and 1250ºC at the base of the model (see Fig. 1). Variations of the following parameters are investigated: (1) the depth of the 1250ºC-isotherm at 150 or 200 km depth, which implies various lithospheric

thicknesses; (2) the radiogenic heat-production rate within the crustal layer (see also Section 4.1.1); and (3) different assumptions of the thermal conductivity distribution (see also Section 4.1.1). All petrophysical parameters correspond to the values given in Table 1.

4.3.2. Model results

Two families of steady-state, one-dimensional geotherms (corresponding to the varied lithospheric thicknesses) and the resulting surface heat-flow density for the Andean foreland are shown in Fig. 5. Modelled geotherms are very similar with those presented by Chapman and Furlong (1992) for stable shield areas. Temperatures at the crust/mantle boundary are on the order of 400–600°C; calculated

surface heat-flow density values are within the range of 40–56 mW m^{-2}. Comparisons of modelling results and measured surface heat-flow density (on the order of 40 mW m^{-2}) show that the lithosphere of the Andean foreland can be described as a cold continental lithosphere with a thickness of about 200 km. However, low heat-flow density in the Andean foreland may be affected by transient thermal effects in the uppermost crust. Rapid burial in the last 10 Ma with a subsidence rate of 0.1–0.4 mm a^{-1} (Coudert et al., 1995) may cause non-steady-state conditions because the thermal field must continuously readjust to new surface conditions. The analytical evaluation of the effect of sedimentation can be treated (comparable to the effect of erosion) by the equation of heat conduction in a moving solid (Carslaw and
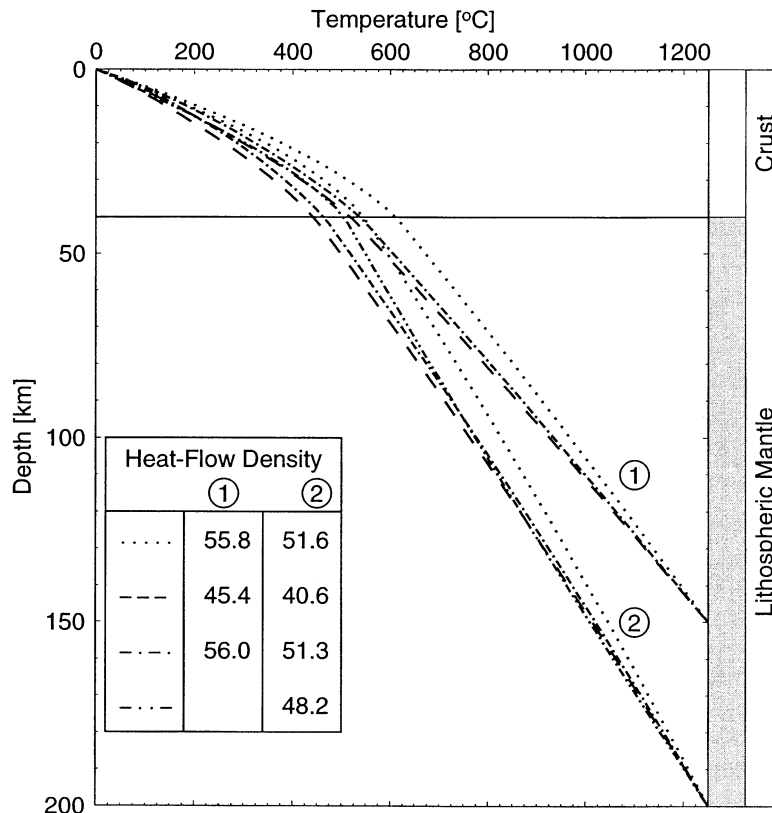

Fig. 5. Lithospheric geotherms calculated for the Andean foreland. One-dimensional, steady-state and conductive heat transfer conditions are assumed. Family of geotherms: *1* corresponds to a lower boundary condition of 1250°C at 150 km depth, and *2* to a lower boundary condition of 1250°C at 200 km depth. Variation of the crustal radiogenic heat production ($\cdots$: $A(z) = $ const. $= 0.9$ μW/m^3; $---$: $A(z) = A_0 \exp(-z/D)$ with $A_0 = 1.5$ μW/m^3; $-\cdot-\cdot$: $A(z) = A_0 e^{-z/D}$ with $A_0 = 3.0$ μW/m^3) and thermal conductivity ($-\cdot\cdot-$: $\lambda(T) = \lambda_0/(1 + cT)$. Resulting surface heat-flow density values (in mW/m^2) according to the geotherms are shown on inset table.

Jaeger, 1959, p. 388). Subsidence rates as estimated by Coudert et al. (1995) may decrease the surface heat-flow density by about 15% (see also Springer and Förster, 1998).

5. Conclusions

A compilation of different modelling results along a W–E profile is shown in Fig. 6. With regard to the varying tectonic regimes in the central Andes the following conclusions can be made.

Model calculations for the fore-arc region suggest low shear stresses along the contact between the oceanic and continental lithosphere. A maximum mean shear stress of 15 MPa resulting in low frictional heat generation rates is considered to be a reasonable value for the subduction regime. Varia-

tions of the subduction angle influence the width and shape of the surface heat-flow density anomaly as well as the heat-flow density level. Shallow subduction results in higher temperatures along the subduction contact and within the overriding continental crust. Modelling shows negligible influence of the subduction velocity on the thermal field in the fore-arc region. Temperatures at the maximum depth of seismic coupling between the oceanic Nazca plate and the overriding South American continental plate (∼45 km) are on the order of 250 to 300°C, whereas at the maximum depth of the plate contact (∼60 km) temperatures are on the order of 300 to 350°C.

Lithospheric temperature conditions of the fore-arc region close to the active magmatic arc are sensitive to the presence of an assumed asthenospheric mantle wedge at shallow depth (∼70 km). To match conditions for melting at subcrustal levels,
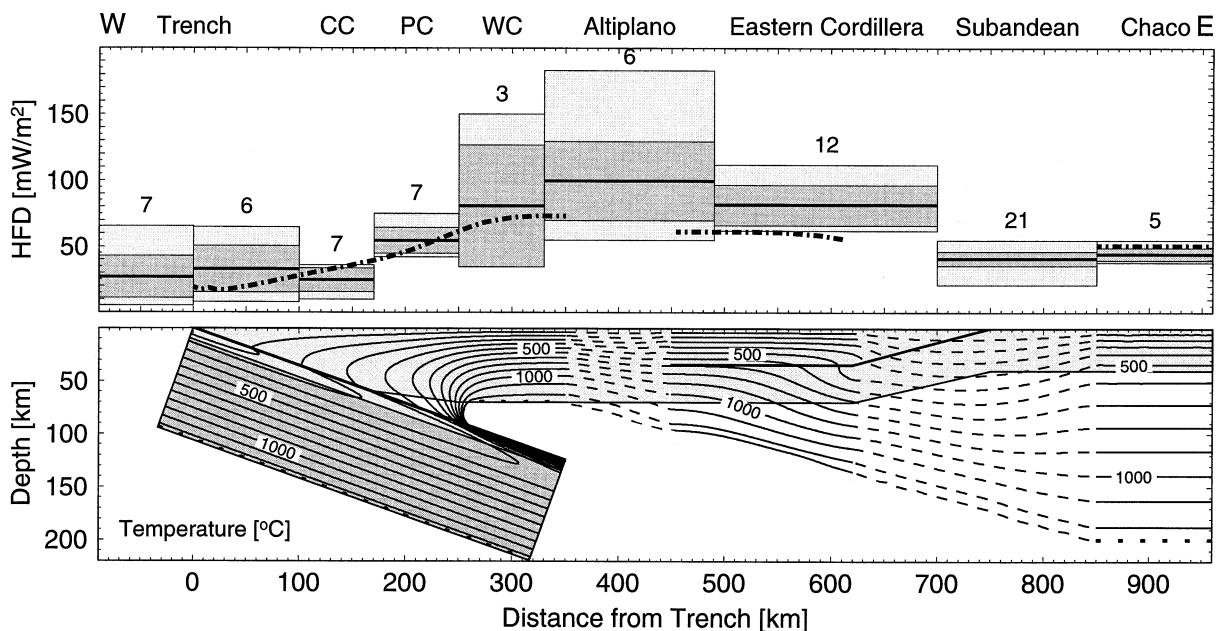

Fig. 6. Compilation of separate model calculations (bottom) along the W–E profile, the resulting surface heat-flow density (dashed/dotted line) and measured heat-flow density (top; see Springer and Förster, 1998). Measured heat-flow data are compiled between 15 and 30°S; shown are mean heat-flow density (black line) for each tectono-morphologic unit, mean absolute deviation (dark shaded range), range between minimum and maximum value (shaded), and number of heat-flow density values determined in each unit. *CC* is Coastal Cordillera, *PC* is Precordillera, and *WC* is Western Cordillera. 1250°C-isotherm: (dotted) used as boundary condition of the models. Between the modelled sections temperatures are extrapolated (dashed isotherms) to the 1250°C-isotherm. Parameters used for the subduction model: case SH2 for the shear stress distribution along the plate contact (see Fig. 2), westward extent of the asthenospheric mantle wedge to the volcanic line (see case MW2 of Fig. 1); crustal stacking model: initial conditions according to the Eastern Cordillera and low shear stress along the thrust (see Fig. 4a); Andean foreland: 1250°C-isotherm at 200 km depth. All other parameters correspond to Table 1.

the minimum extent of the asthenospheric wedge towards the west has to coincide with the position of the volcanic front. The thermally thinned lithosphere results in a surface heat-flow density on the order of 60–70 mW m^{-2}. Locally higher heat-flow density in the volcanic arc is interpreted as the effect of isolated magma chambers located at shallow depth. To explain local anomalies of up to 180 mW m^{-2}, magma chambers at extremely shallow depth of about 4–6 km (top of the chamber) have to be considered. Heat-flow density anomalies caused by isolated magma chambers are extremely short-lived. About 1 Ma after the emplacement, the anomaly diminishes to about 10 mW m^{-2}, which cannot be resolved in the case of the central Andean heat-flow data set.

The subduction models demonstrate the importance of shear stress along the plate contact to the calculated lithospheric thermal field close to the trench. The amount of shear stress is mainly influenced by the coefficient of friction. There is no evidence that parameters influencing the coefficient of friction (e.g. viscosity of subducted sediments or fluids within the subduction channel) have changed significantly during the time of subduction. Thus, the assumption of a uniform frictional heat generation with time seems appropriate. Variations of the subduction angle in the central Andes during time are not well constrained. Comparisons of the present subduction geometry of the central Andes with the flat slab subduction further to the north and south (<16ºS and >28ºS), and the variation of the subduction angle with time there (e.g. Sébrier and Soler, 1991; Kay and Abbruzzi, 1996) suggest that the subduction angle may also have changed with time in the central Andes (see discussion in Allmendinger et al., 1997). However, changes from 'normal' subduction to 'flat' subduction occur at greater depths (>100 km, see contours of Wadati–Benioff zone of Cahill and Isacks (1992)), and thus have little effect on the thermal structure in the fore-arc region. The amount of the crustal radiogenic heat production, its vertical distribution and possible variation during the process of subduction are not known. Recent discussions on the vertical distribution of radiogenic heat production are controversial (e.g. discussion by McLennan and Taylor (1996)). Therefore, a constant heat generation rate in the continental crust (with

depth and time) seems to be most reasonable. As a conclusion of these model calculations, steady-state conditions for the fore-arc region close to the trench seem to be justified. Further to the east, close to the volcanic arc, the situation is more complicated and temporal changes of subduction geometry have to be taken into account. Variations in the subduction angle at greater depths influence the development of an asthenospheric mantle wedge. In the situation of the central Andes a 'present day' asthenospheric mantle wedge has to be assumed to satisfy temperature conditions for melting at subcrustal levels and extensive volcanism. In the case of flat subduction, no asthenospheric mantle wedge is existent and the cooling effect of the subduction process results in very low temperatures. Furthermore, the development of the modern central Andes involved major crustal thickening and uplift since the Late Oligocene (Gubbels et al., 1993; Allmendinger et al., 1997; Jordan et al., 1997; Okaya et al., 1997). Therefore, non-uniform subduction parameters should be considered and temperature calculations, assuming steady-state conditions in the region of the volcanic arc, can be used only for general approximations.

The main results of the modelling can be summarised as follows. The existence of an asthenospheric mantle wedge results in only a slight increase of surface heat-flow density, to a maximum of about 70 mW m^{-2}. A sharp increase in heat-flow density, as observed in other subduction zones such as in the North American Cascades (Blackwell et al., 1982; Lewis et al., 1988) and in the Tohoku arc of Japan (Honda, 1985) cannot be explained by the subduction process itself. Heat-flow density in the region of the volcanic arc and Altiplano can be explained by two components: a background heat-flow density resulting from the subduction process and a second one resulting from near-surface heat sources (e.g. magma chambers).

The continental crust of the volcanic arc and Altiplano is characterised by various geophysical anomalies: anomalously low seismic velocities in the deeper crust (Wigger et al., 1994), the general absence of crustal earthquakes (Cahill and Isacks, 1992), the high seismic wave attenuation (Graeber and Haberland, 1997), a major negative Bouguer anomaly (Götze and Kirchner, 1996) and a zone of extremely high electrical conductivities (Schwarz

and Krüger, 1997). The existence of an astheno-spheric mantle wedge at shallow depth leads to high crustal temperatures in the volcanic arc and Altiplano region. The temperature calculations support the interpretation of the geophysical anomalies as large areas of partial melts in the deeper crust (Schmitz et al., 1997).

The lithospheric thermal structure of the back-arc region is strongly influenced by the crustal stacking process. However, reverse temperature–depth distributions in the continental crust do not result in 2-D crustal stacking models. The recent lithospheric thermal structure is mainly influenced by the initial temperature distribution assumed at the beginning of the crustal stacking process. The lithospheric thermal structure of the back-arc region can be explained by a transition from a lithosphere/asthenosphere boundary at shallow depth to a 'normal' lithospheric thickness for continental shields. Thus, the proposed lithospheric structure for the central Andes, with a thinned lithosphere beneath the Western Cordillera, Altiplano and western part of the Eastern Cordillera, is similar to that proposed previously by Isacks (1988) and Lamb et al. (1997), but differs from that of Whitman et al. (1992). Melting temperatures in the lower crust (crust/mantle transition at about 70 km depth) result in a maximum surface heat-flow density on the order of 60 mW m^{-2}. An increase of surface heat-flow density by an increased heat production rate resulting from crustal doubling cannot be observed 10 Ma after the onset of thrusting. Higher surface heat-flow density in the area of the Eastern Cordillera may be attributed to transient effects on the thermal field by erosional processes, which were not considered in the numerical models.

The observed surface heat-flow density in the Andean foreland (Chaco) can be explained by lithospheric thermal conditions corresponding with those of typical shield areas. Temperature estimates at the crust/mantle transition are on the order of 400 to 600ºC considering a lithospheric thickness of 150–200 km. However, the low surface heat-flow density in the area of the Andean foreland may be attributed to transient effects in the thermal field caused by recent sedimentation.

References

Allmendinger, R.W., Jordan, T.E., Mahlburg-Kay, S., Isacks, B.L., 1997. The evolution of the Altiplano–Puna Plateau of the Central Andes. Annu. Rev. Earth Planet. Sci. 25, 139–174.

Anderson, R.N., Langseth, M.G., Vacquier, V., Francheteau, J., 1976. New terrestrial heat flow measurements on the Nazca Plate. Earth Planet. Sci. Lett. 29, 243–254.

Andrews, D.J., Sleep, N.H., 1974. Numerical modelling of tectonic flow behind island arcs. Geophys. J. R. Astron. Soc. 38, 237–251.

Beck, S.L., Zandt, G., Myers, S.C., Wallace, T.C., Silver, P.G., Drake, L., 1996. Crustal thickness variations in the central Andes. Geology 24, 407–410.

Blackwell, D.D., Bowen, R.G., Hull, D.A., Riccio, J., Steele, J.L., 1982. Heat flow, arc volcanism, and subduction in northern Oregon. J. Geophys. Res. 87, 8735–8754.

Cahill, T., Isacks, B.L., 1992. Seismicity and shape of the subducted Nazca Plate. J. Geophys. Res. 97, 17503–17529.

Cande, S.C., Haxby, W.F., 1991. Eocene propagating rifts in the Southwest Pacific and their conjugate features on the Nazca Plate. J. Geophys. Res. 96, 19609–19622.

Carslaw, H.S., Jaeger, J.C., 1959. Conduction of Heat in Solids. Oxford Science Publications, Clarendon Press, Oxford, 2nd ed.

Čermák, V., Haenel, R., 1988. Geothermal maps. In: Haenel, R., Rybach, L., Stegena, L. (Eds.), Handbook of Terrestrial Heat-Flow Density Determination. Kluwer, Dordrecht, pp. 261–300.

Čermák, V., Rybach, L., 1982. Thermal Conductivity and Specific Heat of Mineral and Rocks. In: Angenheister, G. (Ed.), Landolt–Börnstein — Numerical Data and Functional Relationships in Science and Technology, Vol. 1. Physical Properties of Rocks. Springer, Berlin, pp. 305–343.

Chapman, D.S., Furlong, K.P., 1992. Thermal state of the continental lower crust. In: Fountain, D.M., Arculus, R., Kay, R.W. (Eds.), Continental Lower Crust. Developments in Geotectonics 23, Elsevier, Amsterdam, pp. 179–199.

Clauser, C., Huenges, E., 1995: Thermal Conductivity of Rocks and Minerals. In: Ahrens, T.J. (Ed.), Handbook of Physical Constants. American Geophysical Union, Washington D.C., pp. 105–126.

Coira, B., Davidson, J., Mpodozis, C., Ramos, V., 1982. Tectonic and magmatic evolution of the Andes of northern Argentina and Chile. Earth Sci. Rev. 18, 303–332.

Comte, D., Suárez, G., 1995. Stress distribution and geometry of the subducting Nazca plate in northern Chile using teleseismically recorded earthquakes. Geophys. J. Int. 122, 419–440.

Coudert, L., Frappa, M., Viguier, C., Arias, R., 1995. Tectonic subsidence and crustal flexure in the Neogene Chaco basin of Bolivia. Tectonophysics 243, 277–292.

Crough, S.T., 1983. Apatite fission-track dating of erosion in the eastern Andes, Bolivia. Earth Planet. Sci. Lett. 64, 396–397.

Davies, J.H., Stevenson, D.J., 1992. Physical model of source regions of subduction zone volcanics. J. Geophys. Res. 97, 2037–2070.

DeMets, C., Gordon, R.G., Argus, D.F., Stein, S., 1990. Current plate motions. Geophys. J. Int. 101, 425–478.

Dumitru, T.A., 1991. Effects of subduction parameters on geothermal gradients in forearcs, with an application to Franciscan subduction in California. J. Geophys. Res. 96, 621–641.

Favetto, A., Martinelli, P., Osella, A., 1997. Electrical and thermal anomalies in the Central Andean subduction zone. Pure Appl. Geophys. 149, 391–404.

Francis, P.W., Hawkesworth, C.J., 1994. Late Cenozoic rates of magmatic activity in the Central Andes and their relationship to continental crust formation and thickening. J. Geol. Soc. London 151, 845–854.

Froidevaux, C., Isacks, B.L., 1984. The mechanical state of the lithosphere in the Altiplano–Puna segment of the Andes. Earth Planet. Sci. Lett. 71, 305–314.

Furukawa, Y., 1993. Depth of the decoupling plate interface and thermal structure under arcs. J. Geophys. Res. 98, 20005–20013.

Germann, D., 1990. Thermische und strukturelle Prozesse in der Überschiebungstektonik und ihre numerische Behandlung. Ph.D. thesis, Technische Universität Clausthal.

Giese, P., 1994. Geothermal structure of the Central Andean crust — implications for heat transport and rheology. In: Reutter, K.-J., Scheuber, E., Wigger, P. (Eds.), Tectonics of the Southern Central Andes. Springer, Berlin, pp. 69–76.

Götze, H.-J., Kirchner, A., 1996. Interpretation of gravity and geoid in the central Andes between 20° to 29°S. J. South Am. Earth Sci. 10, 179–188.

Graeber, F.M., Haberland, C., 1997. Travel time and attenuation tomography with local earthquake data from the PISCO Experiment in Northern Chile. Eos 77, 646.

Gubbels, T.L., Isacks, B.L., Farrar, E., 1993. High-level surfaces, plateau uplift, and foreland development, Bolivian central Andes. Geology 21, 695–698.

Haenel, R., Mongelli, F., 1988. Thermal exploration methods. In: Haenel, R., Rybach, L., Stegena, L. (Eds.), Handbook of Terrestrial Heat-Flow Density Determination. Kluwer, Dordrecht, pp. 353–389.

Hamza, V., Muñoz, M., 1996. Heat flow map of South America. Geothermics 25, 599–646.

Henry, S.G., 1981. Terrestrial Heat Flow Overlying the Andean Subduction Zone. Ph.D. thesis, Univ. of Michigan, Ann Arbor, MI.

Henry, S.G., Pollack, H.N., 1988. Terrestrial heat flow above the Andean subduction zone in Bolivia and Peru. J. Geophys. Res. 93, 15153–15162.

Honda, S., 1985. Thermal structure beneath Tohoku, northeast Japan — a case study for understanding the detailed thermal structure of the subduction zone. Tectonophysics 112, 69–102.

Hyndman, R.D., Wang, K., 1993. Thermal constraints on the zone of major thrust earthquake failure: the Cascadia subduction zone. J. Geophys. Res. 98, 2039–2060.

Hyndman, R.D., Wang, K., 1995. Thermal constraints on the seismogenic portion of the southwestern Japan subduction thrust. J. Geophys. Res. 100, 15373–15392.

Isacks, B.L., 1988. Uplift of the Central Andean Plateau and bending of the Bolivian Orocline. J. Geophys. Res. 93, 3211–3231.

Jordan, T.E., Gardeweg, M., 1989. Tectonic evolution of the Late Cenozoic Central Andes (20°–33°S). In: Ben-Avraham, Z. (Ed.), The Evolution of the Pacific Ocean Margins. Oxford University Press, New York, pp. 193–207.

Jordan, T.E., Reynolds, H.J., III, Erikson, J.P., 1997. Variability in age of initial shortening and uplift in the Central Andes, 16–33° 30′S. In: Ruddiman, W.F. (Ed.), Tectonic Uplift and Climatic Change. Plenum Press, New York, pp. 41–61.

Kay, S.M., Abbruzzi, J.M., 1996. Magmatic evidence for Neogene lithospheric evolution of the central Andean 'flat-slab' between 30°S and 32°S. Tectonophysics 259, 15–28.

Kirby, S.H., 1983. Rheology of the lithosphere. Rev. Geophys. Space Phys. 21, 1458–1487.

Kirby, S.H., Okal, E.A., Engdahl, E.R., 1995. The 9 June 94 Bolivian deep earthquake: an exceptional event in an extraordinary subduction zone. Geophys. Res. Lett. 22, 2233–2236.

Kudrass, H.-R., Delisle, G., Goergens, A., Heeren, F., von Huene, R., Jensen, A., Kawohl, H., Kiefer, E., Kohler, I., Marchig, V., Marzan, I., Naumann, R., Poggenburg, J., von Rad, U., Rask, H., Roetzler, K., Seyfried, H., Steinmann, D., Teschner, M., Weinrebe, W., Wissmann, G., Wilke, H.-G., Ye, S., 1995. Crustal Investigations Off- and Onshore, Nazca/Central Andes (CINCA). Report Sonne-Cruise 104, LEG3, BGR114281, Bundesanstalt für Geowissenschaften und Rohstoffe, Hannover.

Lamb, S., Hoke, L., Kennan, L., Dewey, J., 1997. Cenozoic evolution of the Central Andes in Bolivia and northern Chile. In: Burg, J.-P., Ford, M. (Eds.), Orogeny Through Time. Geol. Soc. Spec. Publ. 121, 237–264.

Lewis, T.J., Bentkowski, W.H., Davies, E.E., Hyndman, R.D., Souther, J.G., Wright, J.A., 1988. Subduction of the Juan de Fuca Plate: thermal consequences. J. Geophys. Res. 93, 15207–15225.

McLennan, S.M., Taylor, S.R., 1996. Heat flow and the chemical composition of the continental crust. J. Geol. 104, 369–377.

Molnar, P., England, P., 1990. Temperature, heat flux, and frictional stress near major thrust faults. J. Geophys. Res. 95, 4833–4856.

Molnar, P., England, P., 1995. Temperatures in zones of steady-state underthrusting of young oceanic lithosphere. Earth Planet. Sci. Lett. 131, 57–70.

Müller, R.D., Roest, W.R., Royer, J.-Y., Gahagan, L.M., Sclater, J.G., 1997. Digital isochrons of the world's ocean floor. J. Geophys. Res. 102, 3211–3214.

Muñoz, M., 1987. Flujo de calor en Chile con enfasis en las areas de El Tatio de La Cuenca de Santiago. Rev. Bras. Geofis. 5, 153–164.

Muñoz, M., Hamza, V., 1993. Heat flow and temperature gradients in Chile. In: Čermák, V. (Ed.), Proceedings of the International Meeting on Terrestrial Heat Flow and the Lithosphere Structure, Bechyne Castle. Stud. Geophys. Geod. 37, 315–348.

Okaya, N., Tawackoli, S., Giese, P., 1997. Area-balanced model of the late Cenozoic tectonic evolution of the central Andean arc and back arc (lat. 20°–22°S). Geology 25, 367–370.

Pardo-Casas, F., Molnar, P., 1987. Relative motion of the Nazca (Farallon) and South American Plates since Late Cretaceous time. Tectonics 6, 233–248.

Peacock, S.M., 1989. Thermal modeling of metamorphic pressure–temperature–time paths: a forward approach. In: Spear, F.S., Peacock, S.M. (Eds.), Metamorphic Pressure–Temperature–Time Paths. Short Course in Geology 7, AGU, Washington, D.C., pp. 57–102.

Peacock, S.M., 1993. Large-scale hydration of the lithosphere above subducting slabs. Chem. Geol. 108, 49–59.

Pollack, H.N., Hurter, S., Johnson, R.J., 1993. Heat flow from the Earth's interior — analysis of the global data set. Rev. Geophys. 31, 267–280.

Roeder, D., 1988. Andean-age structure of Eastern Cordillera (Province of La Paz). Tectonics 7, 23–39.

Scheuber, E., Bogdanic, T., Jensen, A., Reutter, K.-J., 1994. Tectonic development of the North Chilean Andes in relation to plate convergence and magmatism since the Jurassic. In: Reutter, K.-J., Scheuber, E., Wigger, P. (Eds.), Tectonics of the Southern Central Andes. Springer, Berlin, pp. 121–139.

Schmitz, M., 1994. A balanced model of the southern Central Andes. Tectonics 13, 484–492.

Schmitz, M., Kley, J., 1997. The geometry of the Central Andean backarc crust: joint interpretation of cross-section balancing and seismic refraction data. J. South Am. Earth Sci. 10, 99–110.

Schmitz, M., Heinsohn, W.-D., Schilling, F.R., 1997. Seismic, gravity and petrological evidence for partial melt beneath the thickened Central Andean crust (21–23°S). Tectonophysics 270, 313–326.

Schwarz, G., Krüger, D., 1997. Resistivity cross section through the southern central Andes as inferred from magnetotelluric and geomagnetic deep sounding. J. Geophys. Res. 102, 11957–11978.

Sclater, J.G., Vacquier, V., Rohrhirsch, J.H., 1970. Terrestrial heat flow measurements on Lake Titicaca, Peru. Earth Planet. Sci. Lett. 8, 45–54.

Sébrier, M., Soler, P., 1991. Tectonics and magmatism in the Peruvian Andes from late Oligocene time to the Present. In: Harmon, R.S., Rapela, C.W. (Eds.), Andean Magmatism and Its Tectonic Setting. Geol. Soc. Am. Spec. Pap. 265, 259–278.

Shi, Y., Wang, C.-Y., 1987. Two-dimensional modeling of the P–T–t paths of regional metamorphism in simple overthrust terrains. Geology 15, 1048–1051.

Springer, M., 1997. Die regionale Oberflächenwärmeflußdichte-Verteilung in den zentralen Anden und daraus abgeleitete Temperaturmodelle der Lithosphäre (with English and Spanish abstracts). Sci. Tech. Rep. STR97/05, GeoForschungsZentrum Potsdam.

Springer, M., Förster, A., 1998. Heat-flow density across the Central Andean subduction zone. Tectonophysics 291, 123–139.

Suárez, G., Comte, D., 1993. Comment on 'Seismic Coupling Along the Chilean Subduction Zone' by B.W. Tichelaar and L.R. Ruff. J. Geophys. Res. 98, 15825–15828.

Thorpe, R.S., Francis, P.W., Harmon, R.S., 1981. Andean andesites and crustal growth. Philos. Trans. R. Soc. London 301, 305–320.

Tichelaar, B.W., Ruff, L.J., 1991. Seismic coupling along the Chilean subduction zone. J. Geophys. Res. 96, 11997–12022.

Tichelaar, B.W., Ruff, L.J., 1993a. Depth of seismic coupling along subduction zones. J. Geophys. Res. 98, 2017–2037.

Tichelaar, B.W., Ruff, L.J., 1993b. Reply. J. Geophys. Res. 98, 15829–15831.

Toksöz, M.N., Minear, J.W., Julian, B.R., 1971. Temperature field and geophysical effects of a downgoing slab. J. Geophys. Res. 76, 1113–1138.

Turcotte, D.L., Schubert, G., 1982. Geodynamics, Applications of Continuum Physics to Geological Problems. Wiley, New York.

Uyeda, S., Watanabe, T., 1970. Preliminary report of terrestrial heat flow study in the South American continent; distribution of geothermal gradients. Tectonophysics 10, 235–242.

Uyeda, S., Watanabe, T., 1982. Terrestrial heat flow in western South America. Tectonophysics 83, 63–70.

Uyeda, S., Watanabe, T., Kausel, E., Kubo, M., Yashiro, Y., 1978. Report of heat flow measurements in Chile. Bull. Earthquake Res. Inst. 58, 131–163.

Uyeda, S., Watanabe, T., Ozasayama, Y., Ibaragi, K., 1980. Report of heat flow measurements in Peru and Ecuador. Bull. Earthquake Res. Inst. 55, 55–74.

Van den Beukel, J., Wortel, R., 1988. Thermo-mechanical modelling of arc–trench regions. Tectonophysics 154, 177–193.

Von Herzen, R.P., 1959. Heat-flow values from the south-eastern Pacific. Nature 183, 882–883.

Watanabe, T., Uyeda, S., Guzman Rao, J.A., Cabre, R., Kuronuma, H., 1980. Report of heat flow measurements in Bolivia. Bull. Earthquake Res. Inst. 55, 43–54.

Whitman, D., Isacks, B.L., Chatelain, J.-L., Chiu, J.-M., Perez, A., 1992. Attenuation of high-frequency seismic waves beneath the Central Andean Plateau. J. Geophys. Res. 97, 19929–19947.

Wigger, P.J., Schmitz, M., Araneda, M., Asch, G., Baldzuhn, S., Giese, P., Heinsohn, W.-D., Martínez, E., Ricaldi, E., Röwer,

P., Viramonte, J., 1994. Variation in the crustal structure of the southern Central Andes deduced from seismic refraction investigations. In: Reutter, K.-J., Scheuber, E., Wigger, P. (Eds.), Tectonics of the Southern Central Andes. Springer, Berlin, pp. 23–48.

Yuen, D.A., Fleitout, L., Schubert, G., Froidevaux, C., 1978. Shear deformation zones along major transform faults and subducting slabs. Geophys. J. R. Astron. Soc. 54, 93–119.

Zandt, G., Velasco, A.A., Beck, S.L., 1994. Composition and crustal thickness of the southern Altiplano crust, Bolivia. Geology 22, 1003–1006.

Zoth, G., Haenel, R., 1988. Thermal conductivity. In: Haenel, R., Rybach, L., Stegena, L. (Eds.), Handbook of Terrestrial Heat-Flow Density Determination. Kluwer, Dordrecht, pp. 449–466.